



The Use of a Jet Column with Different Nozzles as a Reactor for Biodiesel Reaction with Crude Palm Oil as Feedstock

Dijan Supramono^{1*}, Bella Nadhillah Rachmania¹, and Nida Adilah¹

¹Chemical Engineering Department, University of Indonesia
Depok 16424, Indonesia

* Corresponding Author: dsupramo@che.ui.ac.id

ABSTRACT

Biodiesel may be produced by trans-esterification reaction of vegetable oil, which transforms triglycerides into alkyl esters as biodiesel and glycerol as a byproduct, in the presence of an alcohol reactant and a acid or base catalyst. The major obstacle of preventing biodiesel commercialisation is low mass transfer rates from methanol into oil phase to achieve high yield due to large difference in fluid viscosities, i.e. low viscosity methanol and high viscosity oil. Many techniques have been proposed to overcome this obstacle, most of which involve high mole ratio of methanol to triglycerides exceeding 6, but none of them utilised fluid mechanic techniques to fix up the obstacle. The present research adopts a finding in fluid mechanic field that notched and tabbed nozzles are capable of intensifying shear stress between 2 different flows, which consequently increases the contact areas of the flows considerably. For this purpose, in the present research, a jet column was utilised as a reactor where the mixture of reactants, i.e. crude palm oil (CPO) and methanol with catalyst NaOH were recirculated and injected downward vertically into the reactor column from a nozzle at the top of reactor. The type of nozzles and the mole ratio of methanol to CPO were varied (3.75:1; 4.5:1; 5.25:1 and 6:1) to investigate their effects on yield and conversion of the reaction conducted for 60 minutes at temperatures 53-58°C. Nozzles used were notched, tabbed and conventional circular nozzles for comparison. The highest conversion and yield of biodiesel were achieved at mole ratio 6:1 attaining respectively 87.2% and 96.8% using notched nozzle, 87.8% and 96.6% using tabbed nozzle and 71.2% and 75.1 % using circular nozzle for comparison. Therefore, using notched and tabbed nozzles can reduce the excess of methanol reactant thus saving its separation cost while producing high yield of biodiesel.

Keyword: crude palm oil, biodiesel, jet column, circular nozzle, notched nozzle, tabbed nozzle

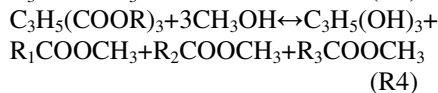
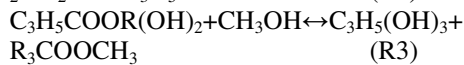
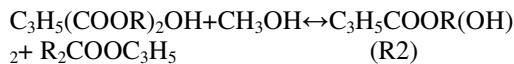
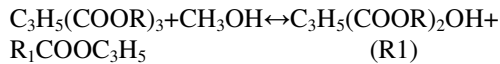
1. INTRODUCTION

The energy demand in Indonesia increases from year to year, especially the demand of transportation fuels. In order to fulfil this demand, Indonesia import fuels more than 77 million barrel in 2012 [1]. One of the means of diminishing import is by the use of fuel alternatives. For diesel fuel, biodiesel can be used as fuel alternative.

The manufacture of biodiesel from vegetable oils can be carried out by converting

triglycerides contained in the vegetable oils to methyl ester as the main component of biodiesel by trans-esterification reaction of oils with alcohol in excess in the present of strong acid or base catalyst [3][4]. One of the potential raw materials for the manufacture is crude palm oil (CPO). At the moment the plantation area for CPO in Indonesia reaches 7.9 million hectares, which produces 23.5 million tonnes of CPO annually. Part of this production, i.e. 16.5 million tonnes, is exported. [2].

The overall process is a sequence of three consecutive and reversible reactions, in which di- and monoglycerides are formed as intermediates [4]. The stoichiometric reaction requires 1 mol of a triglyceride and 3 mol of the alcohol. However, an excess of the alcohol is used to increase the yields of the alkyl esters and to allow its phase separation from the glycerol formed [4]. The three consecutive reactions R1, R2 and R3 and overall reaction R4 are as follows



$\text{C}_3\text{H}_5(\text{COOR})_3$: triglyceride

$\text{C}_3\text{H}_5(\text{COOR})_2\text{OH}$: diglyceride

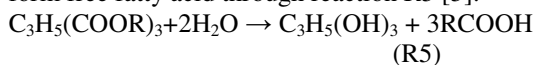
$\text{C}_3\text{H}_5\text{COOR}(\text{OH})_2$: monoglyceride,

CH_3OH : methanol

R_1COOCH_3 , R_2COOCH_3 , R_3COOCH_3 : methyl esters

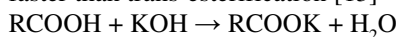
$\text{C}_3\text{H}_5(\text{OH})_3$: glycerine

The reactions in general use methanol in order to produce lower viscosity biodiesel. Water impurity in CPO may react with triglycerides to form free fatty acid through reaction R5 [5].



RCOOH : free fatty acid (FFA).

This produced free fatty acid together with that inherently impures CPO must be kept at small quantity because it can deactivate trans-esterification by reacting with NaOH according to saponification reaction R6. At high FFA content, the kinetics of saponification reaction is faster than trans-esterification [13]



RCOOK : soap

The major obstacle of preventing biodiesel commercialisation is low mass transfer rates from methanol into oil phase to achieve high yield due to large difference in fluid viscosities, i.e. low viscosity methanol and high viscosity oil. In general reactions occur at elevated temperature and ambient pressure to overcome the high viscosity of the vegetable oils to allow the dispersion of the oil in methanol [6]. However, the temperature must be below the

boiling temperature of methanol (64.7°C) to avoid the evaporation and the release of methanol out of the reaction mixture. Alternatively, the reaction is carried out at methanol supercritical conditions [7]. Other means of overcoming this obstacle is by using high mole ratio of methanol to triglycerides exceeding 6 [5]. The high mole ratio renders separation cost of methanol high after the reaction. It also requires larger size of reactor to produce a given amount of biodiesel. Until now none of the biodiesel reactions have explored fluid mechanic techniques to reduce this excess.

The present research adopts a finding in fluid mechanic field that notched and tabbed nozzles are capable of intensifying fluid entrainment and subsequently fluid break-up as a result of shear stress or high velocity gradient between 2 different flows. The break-up of high viscosity oil in the vicinity of low viscosity methanol increases the contact areas between reactants considerably and consequently apparent reaction kinetics.

The shear stress is generated through a turbulence process driven by external forces where an initial energy rate ε_i is transferred to fluid from outside (in the present research from momentum of fluid exiting nozzles) and large-scale vortices are generated [8]. Subsequently an energy rate ε_T is transferred when the vortices break up into smaller scales. At the smallest scales, fluid dissipates heat at the rate ε (see Figure 1). Reaction rate is determined by the smallest scale dynamics. The shapes of a circular nozzle as a reference, notched and tabbed nozzles used in the present research are respectively shown in Figures 2a, 2b and 2c.

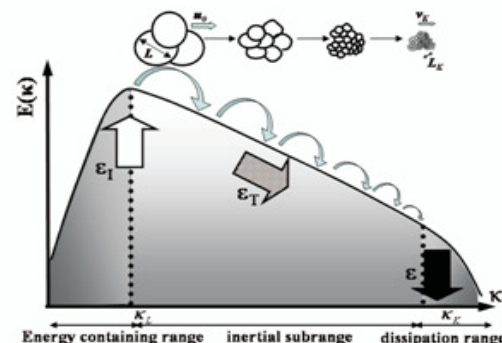


Figure 1. Sketch of the energy cascade [8].



Figure 2a. Circular nozzle



Figure 2b. V-major notched nozzle

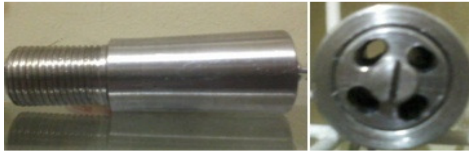


Figure 2c. Tabbed nozzle

Three dimensional sketch of the vortex dynamics in the circular nozzle jet is described in Figure 3. Well-detached K-H rings are continuously displayed in azimuthal direction at different axial positions. Their detaching results in secondary instabilities of the braid (region between two successive rings), which generate streamwise structures [14][15]. It appears that the production of streamwise structures is governed by the K-H rings. Figure 4 shows numerical visualisation of the instantaneous dye concentration distribution in the x - y and x - z planes parallel to the jet axis at time = 64 periodic time in circular nozzle jet [9]. In this figure, the base dimension of the dye distribution is the diameter of the nozzle D . Instability of the vortex sheet of the jet featured by the braid causes roll-up of the vortex sheet and the formation of concentrated vortex rings at the roll-up locations. Starting with the second vortex ring, the dye concentration spread out from the structures at the roll-up locations. The vortex rings induce the ambient fluid immediately upstream of them to move inwards towards the jet axis and the jet fluid immediately downstream to move outwards from the axis indicating fluid entrainment from the ambient into the jet by the vortex rings.

Figure 5 shows the instantaneous dye distribution in the x - y (peak-to-peak) and the x - z (trough-to-trough) meridional planes of the V-nozzle at time = 64 periodic time in the V-major nozzle jet [9]. The spread of the dye in the V-nozzle is significantly greater than that in the circular nozzle. The first vortex ring induces an outward motion of the jet fluid, while the second

vortex ring induces strong entrainment of the ambient fluid towards the jet flow. This counter motion enhances mixing and might also be responsible for the instability of the vortex rings because of the strong shear between them. At $x/D = 2.8$ and 3.8 the dye distributions remain circular. At $x/D = 4.8$ there are six small mushroom-like structures sprouting out from the edge of the circle. They grow larger downstream from $x/D = 5.8$ to 6.8 both at peak and trough locations. This distinct distortion of the originally circular vortex sheet by the notches of the nozzle exit promotes the distortion and subsequent instability of the vortex rings, leading to the creation of strong streamwise vortex pairs at both the peak and trough locations. These vortex pairs induce outward and inward motions of the fluid in different azimuthal regions of the jet and subsequent breakup and smearing of them at $x/D = 6.8$ and 7.8 suggest strong entrainment of the ambient fluid into the jet.

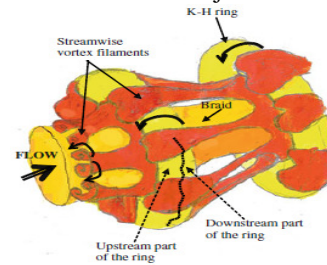


Figure 3. Three dimensional vortex dynamics description of circular nozzle jet [10]

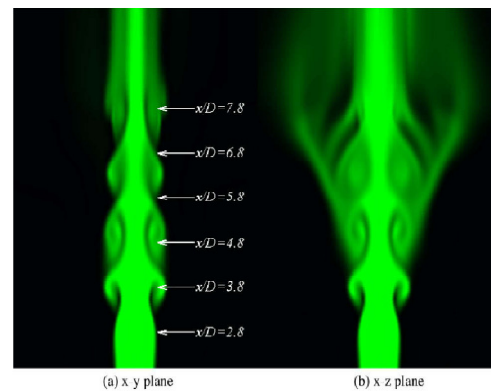


Figure 4. Instantaneous dye concentration in the cross-planes parallel to jet axis for circular nozzle jet at Reynolds number ~ 2800. [9]

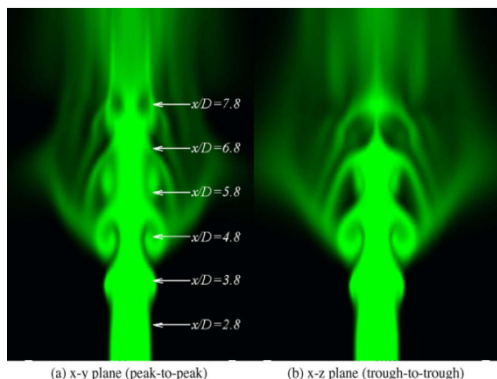


Figure 5. Instantaneous dye concentration in the cross-planes parallel to jet axis for V-major jet at Reynolds number ~ 2800 [9]

In the streamwise plane of the cross-shaped tabbed nozzle jet (see Figure 10a for nozzle configuration), K-H instabilities are observed from about $x/D = 1$ similar to those in the circular nozzle jet. Further downstream, K-H structures start to disintegrate and appear to be K-H ring segments at $x/D = 3$ [12] as shown by transverse plane image in Figure 6. It describes hand-made sketch of three-dimensional organization of the primary (K-H ring segments) and secondary streamwise vortices [10]. Comparison of Figures 3 and 6 shows that in the circular jet (Figure 3) the K-H structure is continuous in azimuthal direction and has a ring shape. The plane which crosses the centre of the K-H structure is considered as the limit between the upstream and the downstream parts of the azimuthal vortex where ambient fluid entrainment is present in the upstream part of the ring. In the downstream part of the ring, the jet expands. For the tabbed nozzle jet (Figure 6), K-H vortices are smaller than in the circular jet and discontinuous in azimuthal direction. On the discontinuity regions, secondary vortices develop and perform entrainment continuously. For comparison for the entrainment, exiting the same nozzle sizes (12mm), circular nozzle jet is surrounded by continuous K-H vortices in azimuthal direction, while tabbed nozzle jet by continuous secondary vortices in streamwise direction (Figure 7). Nastase *et al* confirm that the later vortices yields almost three times greater entrainment than the earlier vortices [12]. In the downstream, the secondary large scale vortices break-up into smaller vortices [11].

2. METHOD

In the present research, a jet column was utilised as a reactor where the mixture of reactants, i.e.

CPO and methanol with catalyst NaOH were recirculated through a centrifugal pump and injected downward vertically into the reactor column from a nozzle at the top of reactor (see Figure 8). The jet velocity was set 4 m/sec. It is expected that the injection will intensify the entrainment of reaction mixture in the column by high velocity jet from the nozzle and break-up of vortices in the lower part of the column. The mole ratio of methanol to CPO were varied (3.75:1; 4.5:1; 5.25:1 and 6:1) to investigate their effects on yield and conversion of the reaction conducted for 60 minutes at temperatures 53-58°C. Nozzles used were notched, tabbed and conventional circular nozzles for comparison. Samples from the jet column were taken after 60 minute reaction and brought to a laboratory for High Performance Liquid Chromatography (HPLC) analysis.

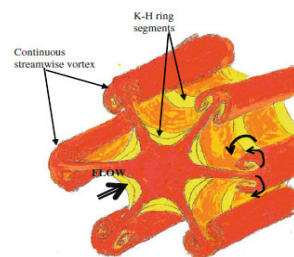


Figure 6. Three dimensional vortex dynamics description of cross-shaped tabbed nozzle jet [10]

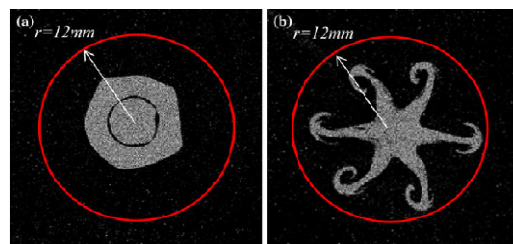


Figure 7. PIV jet transverse section images at $x/D = 3$ with circles being limits of radial velocity averaging, (a) circular nozzle jet (b) cross-shaped tabbed jet at Reynolds number ~ 800 [10]

2.1 HPLC Testing

Samples of CPO and biodiesel from different experimental runs were analyzed by HPLC. It used the Licrosphere column RP18 with moving phase methanol and isopropanol hexane. The detector in HPLC used UV beam of 205 nm wavelength. Yield and conversion percentages were determined based on the analysis results of HPLC. Conversion of CPO

refers to the amount of triglycerides which is converted into diglycerides, monoglycerides and free acid methyl ester (FAME) compared to the amount of triglycerides in CPO by weight, while yield is defined as the amount of FAME compared to the amount of triglycerides in CPO by weight. The conversion was calculated by dividing the total amount of diglycerides, monoglycerides and methyl esters in the biodiesel sample by the total amount of triglycerides, diglycerides, monoglycerides and methyl esters in the biodiesel sample. Yield was calculated by dividing the amount of methyl ester in the biodiesel sample by the amount of triglycerides in CPO sample in the same sample volume.

2.2 Acid Number

Acid number was determined by dissolving 5 grams of the biodiesel sample in 50 ml of alcohol, heating the solution in a water bath. During the heating, the solution was stirred and dripped with phenol phtalein as much as 2% weight of the sample. Then, the sample was being titrated with KOH solution 0.1 N until there was a change of colour from clear to red-purple. The amount of KOH required determined the acid number.

2.3 Water Content

Water content was determined by heating the biodiesel samples put on a beaker glass at 110°C for 30 minutes in an oven.



Figure 8. Experimental rig for biodiesel reactions

3. RESULTS

3.1 Conversions of CPO and yield of methyl esters

The conversions of CPO at different mole ratios of methanol to CPO are shown in Figure 9 and its yields in Figure 10. The earlier figure shows that the higher the mole ratio, the higher is the conversion of CPO to mono-, di-glycerides and methyl esters as expected. Comparison of the results at different types of nozzles demonstrates that at high mole ratio, the conversions are not significantly affected by the types of the nozzles. However, the effect becomes more sensible at lower mole ratios, where the use of notched nozzle results in higher conversion compared to the use of other nozzles. Calculation of Reynolds numbers (Re) based on the cross-section opening of the nozzles shows that at the highest mole ratio, Re is approximately 5600, and at the lowest mole ratio approximately 5400. This Re value is higher than Re's for the analysis of the effects of types of nozzles in Section 1. Therefore, the analysis is relevant to the conditions in this research.

The similar effect shown at high mole ratios may be attributed to the confinement of the jet column in which the spread of vortices in the downstream of the jet for all nozzles is confined by the jet column wall. The blockage ratio of the present column is about 7.5%. Schneider [17] and Hussein *et al* [18] have identified that confined jets cannot entrain fluid through the surrounding walls which results in fluid being is drawn upstream in the ambient flow region. This condition impedes the entrainment and therefore obstructing the reactant mixing.

At lower mole ratios, the viscosity of the reactant mixture is higher which reduces the spread of the vortices and the effect of confinement. In this regime, the effect of nozzle types on the conversion is more apparent. The reason why the conversion resulting from the use of the tabbed nozzle is lower than that using notched nozzle can be traced from the shape of the tabbed nozzle. As shown in Figure 2c, the shape of the nozzle is similar to clover one (Figure 10b) rather than cross one (Figure 10a). Meslem and Nastase [16] found that entrainment in clover-shaped nozzle jet is about a half that in cross-shaped nozzle jet. The inability of clover-shaped nozzle to carry out high entrainment is attributed to the emergence of pairs of vortices near the centre of the nozzle which expel the flow outwards and reduce the entrainment of surrounding fluid inwards (see Figure 11b).

However, in cross-shaped nozzle jet, entrainment into the jet is not hindered by the fluid expulsion

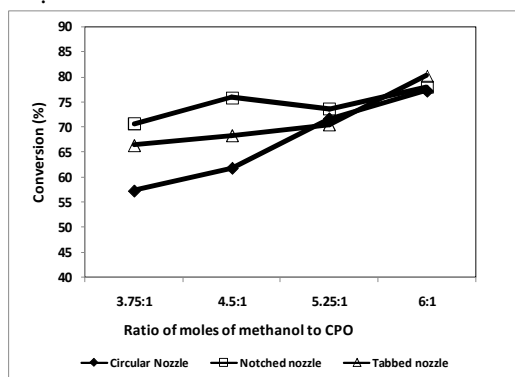


Figure 9. Conversion of CPO at different mole ratios and types of nozzles

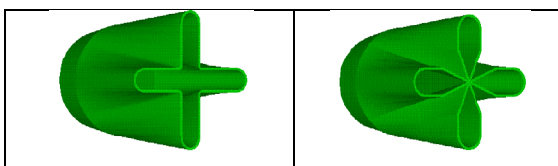


Figure 10a
Configuration of cross-shaped tabbed nozzle

Figure 10b.
Configuration of cross-shaped tabbed nozzle

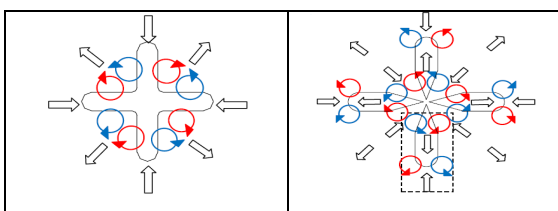


Figure 11a. Pairs of vortices which govern entrainment and expulsion of fluid in cross-shaped nozzle

Figure 11b. Pairs of vortices which govern entrainment and expulsion of fluid in clover-shaped nozzle

Figures 12 shows that both notched and tabbed nozzles affect equally on the conversion of CPO to methyl esters. Eventhough at high mole ratios, they exhibit the similar conversion to combined mono-, methyl esters as shown in Figure 9, the circular nozzle jet produces lower yield of methyl esters. In terms of the length of carbon chains, methyl esters have the shortest molecules compared to other fragmented molecules of CPO, i.e. tri-, di-, and mono-glycerides (see reaction R1, R2, and R3). In other words, methyl esters have the lowest viscosity. Both notched and tabbed nozzles due to exhibiting higher shear compared to the circular nozzle may give more heat dissipation, which is more easily convected in lower viscosity environment in the presence of methyl

esters, which triggers more conversion to methyl esters. It seems that effect of the heat dissipation on the conversion to methyl esters outweighs the effect of entrainment.

3.2 Acid Number in Biodiesel Products

The acid number in biodiesel is an indicator of the content of free fatty acids, which may already be available in CPO or as a side product of reaction R5. The results of acid number for biodiesel products are shown in Table 1.

Table 1. Acid Number in Biodiesel Product

Mole ratio	Acid Number(mg KOH/g oil)		
	Circular	Notched	Tabbed
3.75:1	0.224	0.224	0.336
4.5:1	0.280	0.336	0.392
5.25:1	0.392	0.392	0.392
6:1	0.392	0.392	0.224

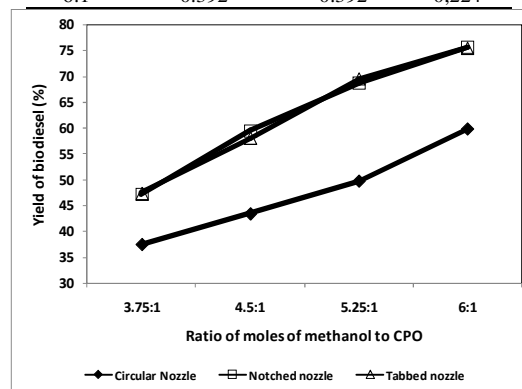


Figure 12. Yield of methyl esters at different mole ratios and types of nozzles

Biodiesel product sampled from the jet column reactor shows the value of acid number is still below the maximum allowable acid number of existing standards either SNI or ASTM D664, i.e. 0.8 mg KOH/gr. This suggests that in terms of acid number, biodiesel produced from the jet column reactor is acceptable to be used as fuel.

Table 1 shows that acid number in biodiesel tends to slightly increase with increasing mole ratio and level off at mole ratio of 6:1, except at tabbed nozzle jet but with small increment. Singh *et al* [19] found the effect of mole ratio of methanol to CPO on FFA conversion using canola oil is arbitrary, when the mole ratio is increases from 3:1 to 4.5:1, the content of FFA is reduced, but it increases when the mole ratio is increased from 4.5:1 to 6:1 with no clear explanation. The obvious effect has been found by Das *et al* (2014) when they worked on *Jatropha curcas* oil [20]. They found that by



increasing mole ratio from 3:1 to 12:1, there is significant increase of FFA conversion from 40% to 92% (and therefore significant reduction of FFA), and infinitesimal increase when the mole ratio is increased further. This conversion will affect the remaining FFA in the biodiesel product. However, the present research exhibits no significant effect. This may occur due to different methods of FFA conversion between that used in the present research and by Das *et al.* In the present research, FFA is reduced using base catalyst, while in Das *et al* research, reduction was carried out using acid catalyst. They suggested that biodiesel be carried out in 2 stages, FFA reduction using acid catalyst, followed by biodiesel reaction using base catalyst.

3.3 Water Content in Biodiesel Products

In trans-esterification reaction mechanism, a small amount of water produced can cause soap formation during the process [5] according to reaction R5 and R6. The maximum allowable water content in biodiesel is 0.05% by weight based on ASTM D 6751 standard for biodiesel and ASTM D 93 for diesel. The results obtained in this study shows that the concentration is still slightly higher than 0.05%. The low water content is important to control the saponification reaction which impairs the quality of biodiesel. It also shifts the equilibrium reaction of biodiesel to the left so that it reduces the CPO conversion to biodiesel.

These higher water contents may be overcome by improving procedure of water removal. In the present research, 1% weight of anhydrous Na_2SO_4 has been used to remove water, but it still cannot suppress the content. Some stages of water removal using anhydrous Na_2SO_4 is required to achieve allowable water content.

Tabel 2. Water Content in Biodiesel Product

Mole ratio	Water Content (%)		
	Circular nozzle	Notched nozzle	Tabbed nozzle
3.75:1	0.183	0.116	0.110
4.5:1	0.231	0.110	0.124
5.25:1	0.124	0.121	0.103
6:1	0.147	0.117	0.107

4. CONCLUSIONS

1. The highest conversion of CPO and yield of biodiesel are achieved at mole ratio 6:1 attaining respectively 77.9% and 75.3% using notched nozzle, 77.2% and 75.6%

using tabbed nozzle and 77.3% and 59.8% using circular nozzle.

2. The confinement of the jet column makes the conversion of CPO independent of the types of nozzles.
3. Higher mole ratio, which is favourable for CPO conversion, adversely increases the content of FFA in biodiesel

REFERENCES

- [1]. M. Mathiyazhagan, M. & A. Ganapathi, "Factor affecting biodiesel production", Bharathidasan University, Department of Biotechnology, May 1, 2011
- [2]. Joelianingsih, H. Maeda, S. Hagiwara, H. Nabetani, Y. Sagara, T.H. Soerawidjaya, A.H. Tambunan, K. Abdullah, "Biodiesel fuels from palm oil via non-catalytic transesterification in a bubble column reactor at atmospheric pressure: A kinetic study", Renewable Energy, vol. 33, pp. 1629-1626, 2007
- [3]. H.J. Wright, J.B. Segur, H.V. Clark, S.K. Coburn, E.E. Langdon, E.N. DuPuis, Oil & Soap, p. 145, 1944.
- [4]. B. Freedman, R.O. Butterfield, E.H. Pryde, J. Am.Oil Chem. Soc., vol. 63, p. 1375, 1986.
- [5]. Jiuxu Liu, "Biodiesel Synthesis via trans-esterification reaction in supercritical methanol: a) A kinetic study, b) Biodiesel Synthesis using microalgae oil", MSc theses, Syracu University, 2013.
- [6]. R. Alcantara, J. Amores, L., Canoira, E. Fidalgo, M.J. Franco, & A. Navarro, "Catalytic production of biodiesel from soy-bean oil, used frying oil and tallow", Biomass & Bioenergy, 18(6), 515-527, 2000.
- [7]. K. Bunyakiat, S. Makmee, R. Sawangkeaw and S. Ngamprasertsith, "Continuous production of biodiesel via transesterification from vegetable oils in supercritical methanol", Energy & Fuels, 20(2), 812-817, 2006.
- [8]. Pierre Sagaut, Sebastien Deck, Marc Terracol, "Multiscale and multiresolution approaches in turbulence", Imperial College Press, 2006.
- [9]. Jinsheng Cai, Her Mann Tsai, Feng Liu, "Numerical simulation of vortical flows in the near field of jets from notched circular nozzles", Computers & Fluids, 39, 539-552, 2010.
- [10]. A. Meslem, M. El Hassan, I. Nastase, "Analysis of jet entrainment mechanism in the transitional regime by time-resolved PIV", J. Visualization, 14:41-52, 2011.
- [11]. Hu Hui, Tetsuo Saga, Toshio Kobayashi, and Nubuyuki Taniguchi, "Simultaneous measurements of all three components of velocity and vorticity vectors in a lobed jet flow by means of dual-plane stereoscopic particle image velocimetry", Phys. Fluids, 14, 2128-2138, 2002.
- [12]. Amina Meslem, Philippe Gervais, Ilinca Nastase, "Primary and secondary vortical structures contribution in the entrainment of low Reynolds number jet flows", Exp Fluids, 44:1027-1033, 2008.
- [13]. J. Van Gerpen, "Biodiesel Production Technology", National Renewable Energy Laboratory, U.S. Department of Energy, Research Report, 2004
- [14]. D. Liepmann, M. Gharib, "The role of streamwise vorticity in the near field entrainment of round jets", J Fluid Mech 245:642-668, 1992.
- [15]. R. Suprayan, H.E. Fiedler, "On streamwise vortical structures in the near-field of axisymmetric shear layers", Meccanica 29(4):403-410, 1994.
- [16]. Amina Meslem, Ilinca Nastase, "Cross and clover shaped orifice jets analysis at low Reynolds number", to



- be submitted to Thermal Science, DOI reference 10.2298/TSC130724166M, 2014.
- [17] W. Schneider, "Decay of momentum flux in submerged jets". J. Fluid Mech. 154:91-110, 1985.
 - [18] H. Hussein, S. Capp, W. George, "Velocity measurements in a high-Reynolds-number momentum conserving, axisymmetric, turbulent jet", J. Fluid Mech. 258:31-75, 1994.
 - [19] A. Singh, B. He, J. Thompson, J. Van Gerpen, "Process optimisation of biodiesel production using alkaline catalyst, Applied Eng. in Agriculture, Vol. 22(4): 597-600, 2006
 - [20] Subrata Das, Ashim Jyoti Thakur, and Dhanapati Deka, "Two-stage conversion of high FFA *Jatropha curcas* oil to biodiesel using Brønsted acidic ionic liquid and KOH as catalysts", Hindawi Publishing Corporation, Scientific World Journal, ID 180983, 2014.